

A EUROPEAN JOURNAL

# CHEMPHYSICHEM

OF CHEMICAL PHYSICS AND PHYSICAL CHEMISTRY



## Reprint

© Wiley-VCH Verlag GmbH & Co. KGaA, Weinheim

A EUROPEAN JOURNAL

# CHEMPHYSICHEM

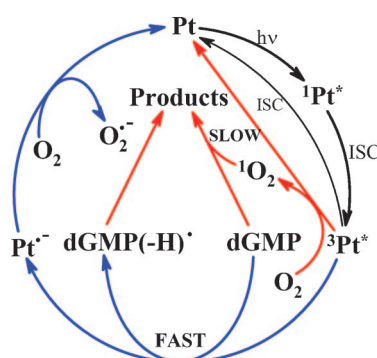
OF CHEMICAL PHYSICS AND PHYSICAL CHEMISTRY

## Table of Contents

*M. P. Serrano, C. Lorente, C. D. Borsarelli,  
A. H. Thomas\**

2244 – 2252

**Unraveling the Degradation  
Mechanism of Purine Nucleotides  
Photosensitized by Pterins: The Role  
of Charge-Transfer Steps**



**Is singlet oxygen always guilty?** For a reaction in which a photosensitizer generates <sup>1</sup>O<sub>2</sub>, it is generally assumed that the substrate molecule is oxidized by <sup>1</sup>O<sub>2</sub> and that the reaction needs O<sub>2</sub> to take place; the reaction is termed <sup>1</sup>O<sub>2</sub>-mediated oxidation. Evidence is presented that counters this assumption, using the oxidation of 2'-deoxyguanosine 5'-monophosphate (dGMP) photosensitized by pterin (Pt) as an example.

# Unraveling the Degradation Mechanism of Purine Nucleotides Photosensitized by Pterins: The Role of Charge-Transfer Steps

Mariana P. Serrano,<sup>[a]</sup> Carolina Lorente,<sup>[a]</sup> Claudio D. Borsarelli,<sup>[b]</sup> and Andrés H. Thomas\*<sup>[a]</sup>

Photosensitized reactions contribute to the development of skin cancer and are used in many applications. Photosensitizers can act through different mechanisms. It is currently accepted that if the photosensitizer generates singlet molecular oxygen ( $^1\text{O}_2$ ) upon irradiation, the target molecule can undergo oxidation by this reactive oxygen species and the reaction needs dissolved  $\text{O}_2$  to proceed, therefore the reaction is classified as  $^1\text{O}_2$ -mediated oxidation (type II mechanism). However, this as-

sumption is not always correct, and as an example, a study on the degradation of 2'-deoxyguanosine 5'-monophosphate photosensitized by pterin is presented. A general mechanism is proposed to explain how the degradation of biological targets, such as nucleotides, photosensitized by pterins, naturally occurring  $^1\text{O}_2$  photosensitizers, takes place through an electron-transfer-initiated process (type I mechanism), whereas the contribution of the  $^1\text{O}_2$ -mediated oxidation is almost negligible.

## 1. Introduction

A photosensitized reaction is defined as a photochemical alteration occurring in one molecular entity as a result of the initial absorption of radiation by another called a photosensitizer.<sup>[1]</sup> The biological and medical importance of photosensitized reactions is mostly related to their participation in processes involved in the development of skin cancer.<sup>[2]</sup> Most of the incident solar UV energy on Earth's surface corresponds to UVA radiation (320–400 nm), which acts indirectly through reactions driven by both endogenous and exogenous photosensitizers, and is now recognized as a class I carcinogen.<sup>[3]</sup> Moreover, epidemiological evidence has shown that exposure of humans to artificial UVA radiation (e.g. sun lamps and tanning beds) is a major risk factor for melanoma induction.<sup>[4–6]</sup> Nevertheless, photosensitization is also important due to several applications including disinfection<sup>[7,8]</sup> and photodynamic therapy (PDT).<sup>[9,10]</sup>

The chemical changes in biological components resulting from photosensitized reactions can take place through different mechanisms. Energy transfer from the triplet state of the photosensitizer can generate excited states in the target molecule,<sup>[11]</sup> which, in the case of DNA, leads to the formation of pyrimidine dimers as the main DNA lesion.<sup>[12]</sup> Photosensitized oxidations also contribute to biological damage induced by

UVA radiation. These processes involve the generation of radicals (type I), for example, by electron transfer or hydrogen abstraction, and/or the production of singlet molecular oxygen [ $\text{O}_2(^1\Delta_g)$ , denoted throughout as  $^1\text{O}_2$ ; type II].<sup>[13]</sup>

In particular,  $^1\text{O}_2$  is one of the main reactive oxygen species (ROS) responsible for the damaging effects of light on biological systems (photodynamic effects) and plays a key role in the mechanism of cell death in PDT.<sup>[14–17]</sup> Moreover, it is currently accepted that the photosensitized modification of proteins occurs mainly through oxidation by  $^1\text{O}_2$ <sup>[18]</sup> and the reaction of guanine with  $^1\text{O}_2$  that leads to several types of DNA lesion is well documented.<sup>[2]</sup>

For a given photosensitized reaction, if the photosensitizer generates  $^1\text{O}_2$  upon irradiation, the target molecule can be oxidized by this ROS, and the reaction needs  $\text{O}_2$  to take place, then the reaction is assumed to be a  $^1\text{O}_2$ -mediated oxidation (type II mechanism). This assumption seems to be somewhat obvious and trivial. However, in a series of recent studies, we have presented experimental evidence against this assumption. In particular, we have demonstrated that in neutral and acidic media the pterin-photosensitized degradation of biological targets, such as 2'-deoxyguanosine 5'-monophosphate (dGMP), Trp, and Tyr, takes place through an electron-transfer-initiated process; the contribution of oxidation by  $^1\text{O}_2$  is almost negligible.<sup>[19–22]</sup> This behavior contrasts with the fact that pterins are efficient  $^1\text{O}_2$ -photosensitizers and all the biomolecules mentioned react efficiently with  $^1\text{O}_2$ .<sup>[23]</sup> The same behavior was suggested for the photosensitized degradation of dGMP by lumazine.<sup>[24]</sup> In a recent study, we have suggested that the oxidation of Trp, photosensitized by phenalenone—a universal reference for  $^1\text{O}_2$  sensitization<sup>[25–27]</sup>—is initiated by an electron transfer from Trp to the triplet excited state of phenalenone and that  $^1\text{O}_2$  does not significantly contribute.<sup>[28]</sup>

[a] M. P. Serrano, Dr. C. Lorente, Dr. A. H. Thomas  
Instituto de Investigaciones Físicoquímicas Teóricas y Aplicadas (INIFTA)  
Departamento de Química, Facultad de Ciencias Exactas  
Universidad Nacional de La Plata (UNLP), CCT La Plata-CONICET  
Casilla de Correo 16, Sucursal 4, (1900) La Plata (Argentina)  
E-mail: athomas@inifta.unlp.edu.ar

[b] Dr. C. D. Borsarelli  
Laboratorio de Cinética y Fotoquímica (LACIFO)  
Centro de Investigaciones y Transferencia de Santiago del Estero (CITSE-  
CONICET) Universidad Nacional de Santiago del Estero (UNSE)  
Casilla de Correo 23, Bs. As. 252, G4200AQF, Santiago del Estero (Argentina)

Supporting Information for this article is available on the WWW under <http://dx.doi.org/10.1002/cphc.201500219>.

The degradation of dGMP photoinduced by pterins, described in our previous works,<sup>[19,20]</sup> yielded the following experimental facts, which have been also reported for the photosensitization of other substrates mentioned above: 1) the reaction does not take place under anaerobic conditions; 2) the consumption of substrate is faster in air-equilibrated solutions than in O<sub>2</sub>-saturated solutions; 3) the rate of oxidation of a given substrate by <sup>1</sup>O<sub>2</sub> calculated from the value of the corresponding rate constant of the chemical reaction (*k<sub>r</sub>*) is much smaller than the experimental rate of consumption of such a substrate; 4) the rate of the reaction increases in the presence of superoxide dismutase (SOD), an enzyme that catalyzes the conversion of superoxide radical anion (O<sub>2</sub><sup>•-</sup>) into H<sub>2</sub>O<sub>2</sub> and O<sub>2</sub>.<sup>[29]</sup>

Taking into account only points 2 and 3, it is clear that the photosensitized oxidations cannot take place exclusively through a type II mechanism. However, considering our previous results on the photosensitization of dGMP,<sup>[19,20]</sup> several questions remain unanswered: 1) if the photosensitized processes are initiated by an electron-transfer reaction, why do the reactions not occur in the absence of O<sub>2</sub>?; 2) why does <sup>1</sup>O<sub>2</sub> not contribute significantly to the oxidation of the substrates?; finally, 3) why does elimination of O<sub>2</sub><sup>•-</sup>, another ROS, accelerate the degradation of the biological target molecule?

The work described here is aimed to answer those questions and to propose a general mechanism that explains these findings and the behavior previously observed. To achieve these goals and understand the role of radical intermediates, excited states, and ROS in the mechanism of a photosensitized process, we have conducted steady-state and time-resolved studies using pterin (Ptr) as a sensitizer and dGMP as a target molecule.

In aqueous solutions at pH 5.5–6.5, UVA irradiation of Ptr–dGMP only produces excitation of the acidic form of Ptr (*pK<sub>a</sub>* = 7.9;<sup>[30]</sup> Figure 1), which is the predominant species at physiological pH. We chose this photosensitized reaction because Ptr is the parent unsubstituted compound of oxidized pterins, a group of photochemically reactive heterocyclic compounds with well-characterized photochemical and photophysical properties.<sup>[30]</sup> Furthermore, some general features of the Ptr–dGMP system have been reported,<sup>[19]</sup> and the radicals of dGMP are well characterized.<sup>[31,32]</sup>

## 2. Results and Discussion

### 2.1. Steady-State Photolysis Experiments

Figure 2 shows the dGMP consumption measured upon continuous irradiation at 350 nm of aqueous solutions containing Ptr and the nucleotide under different experimental conditions. HPLC analysis of the photolyzed samples showed that, in the experiments lacking oxygen, the dGMP concentration did not decrease. However, the rate of dGMP consumption was much greater in air-saturated than in O<sub>2</sub>-saturated solutions (Figure 2). These results, consistent with the general behavior described in the Introduction, revealed that under our experimental conditions, dissolved O<sub>2</sub> is required for the photosensi-

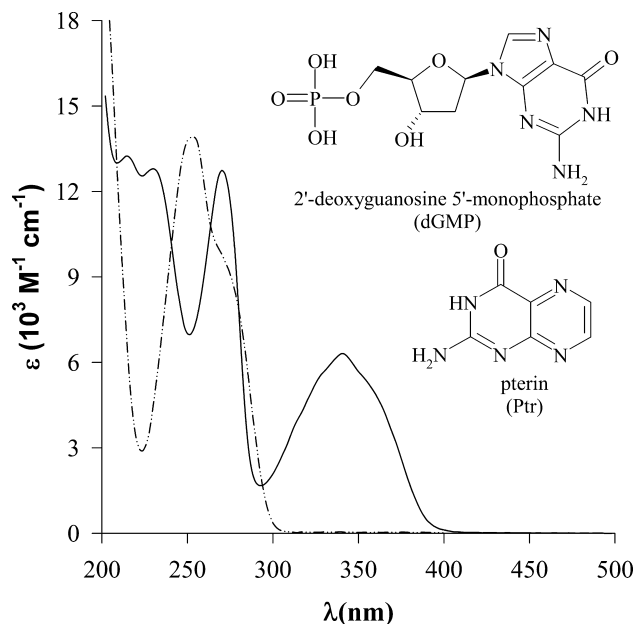


**Figure 1.** Molecular structures of Ptr and dGMP, and the corresponding absorption spectra in air-equilibrated aqueous solutions at pH 5.5; — Ptr, --- dGMP.

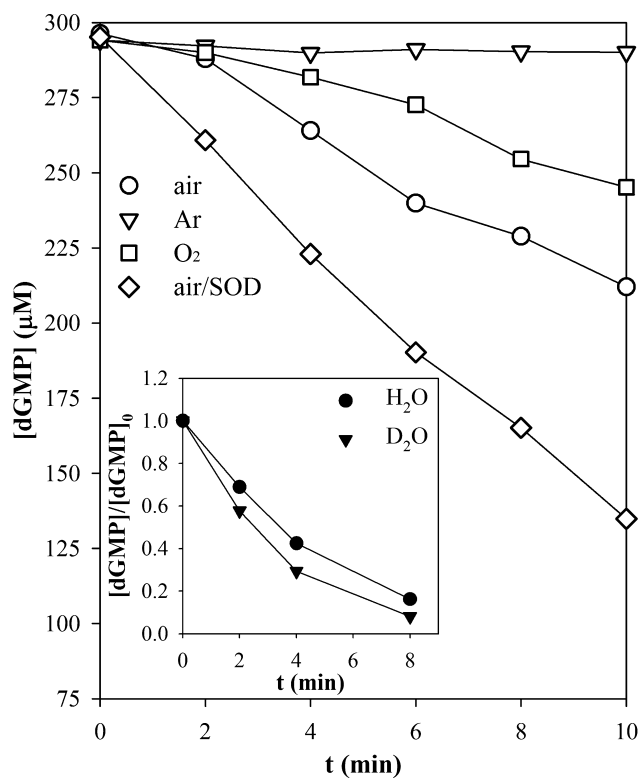


**Figure 2.** Time evolution of the dGMP concentration in aqueous solutions containing Ptr and dGMP as a function of irradiation time. Experiments performed in air-equilibrated solutions in the absence (○) and presence of SOD (◇), in O<sub>2</sub>-saturated (□) and O<sub>2</sub>-free solutions (▽). [Ptr]<sub>0</sub> = 100 μM, [dGMP]<sub>0</sub> = 295 μM, [SOD] = 50 U mL<sup>-1</sup>, pH 5.5. Inset: Comparative experiments carried out in H<sub>2</sub>O (●) and D<sub>2</sub>O (▼); [Ptr]<sub>0</sub> = 150 μM, [dGMP]<sub>0</sub> = 200 μM, pH(pD) 5.5.

tized degradation of dGMP, but that it also inhibits the reaction in high concentrations. Moreover, the presence of SOD caused a significant increase in the rate of dGMP consumption. These results indicate that  $O_2^{\cdot-}$  is involved in the photosensitized process and suggests that the elimination of this ROS inhibits a step that prevents the photosensitized oxidation of dGMP.

In order to confirm the hypotheses proposed (in the Introduction) that  $^1O_2$  plays a negligible or minor role in the Ptr-photosensitized oxidation of dGMP, comparative photolysis experiments were performed in  $H_2O$  and  $D_2O$ . The  $^1O_2$  lifetime in  $D_2O$  is longer than that in  $H_2O$  by a factor of approximately 15 (see the Experimental Section). Air-equilibrated solutions containing Ptr (150  $\mu M$ ) and dGMP (200  $\mu M$ ) in  $H_2O$  and  $D_2O$  at pH/pD 5.5 were irradiated under otherwise identical conditions. The evolution of the absorption spectra and of the concentrations of Ptr and dGMP as a function of the irradiation time (Figure 2, inset) showed that the studied process was not significantly faster in  $D_2O$  than in  $H_2O$  (within experimental error), confirming that  $^1O_2$ -mediated oxidation is not the main pathway of dGMP degradation.

## 2.2. The Excited Triplet States of Ptr

Figure 3 shows the transient absorption spectrum obtained by laser-pulsed excitation at 355 nm of Ar-saturated Ptr solutions (100  $\mu M$ , pH 5.5). The decay of the transient absorption band at 400–550 nm was adjusted using a biexponential fitting function, to yield recovered lifetimes ( $\tau_T$ ) of  $(0.36 \pm 0.08)$  and  $(3.9 \pm 0.7)$   $\mu s$ . This kinetic behavior indicates the existence of, at least two transient absorbing species.<sup>[20]</sup> These two transient species could be assigned to triplet excited states of Ptr based on the following results: 1) increase in the corresponding decay rates in the presence of  $O_2$  (see below), and 2) lifetimes are comparable to those previously reported for the triplet states of Ptr<sup>[33]</sup> and biopterin.<sup>[20,34]</sup> Moreover, it has been proposed that the fast and slow components in the decay of pterins correspond to the simultaneous decay of lactim and lactam tautomers, respectively.<sup>[34,35]</sup>

Ground-state triplet molecular  $O_2$  quenches efficiently both triplet-state tautomers of Ptr, with rate constants of quenching ( $k_{O_2}^T$ ) of  $(5 \pm 1) \times 10^8$  and  $(1.6 \pm 0.3) \times 10^9$   $M^{-1} s^{-1}$  for the short- and long-lived Ptr transient species, respectively, as calculated using the Stern–Volmer equation [Eq. (I)], where  $\tau_T^0$  and  $\tau_T$  are the lifetimes of the triplet states in the absence and presence of the quencher Q ( $O_2$ ; Figure 3 b):

$$\frac{\tau_T^0}{\tau_T} = 1 + \tau_T^0 k_Q^T [Q] \quad (I)$$

## 2.3. Quenching of Ptr Triplet Excited States by dGMP Produces Nucleobase Radicals

It has been reported that dGMP efficiently quenches the triplet excited states of biopterin.<sup>[20]</sup> Figure 4 shows the Stern–Volmer plots [Eq. (I),  $Q = dGMP$ ,  $k_Q^T = k_{dGMP}^T$ ] obtained by laser flash photolysis (LFP) experiments carried out under anaerobic condi-

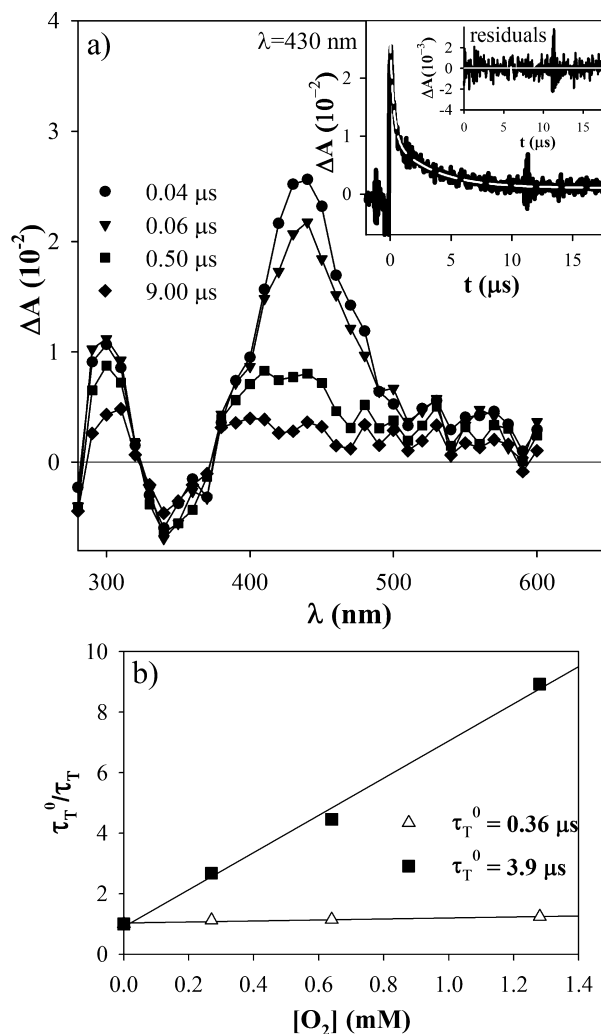


**Figure 3.** a) Differential transient absorption spectra recorded at different times after the 355 nm laser pulse of Ar-saturated aqueous solutions of Ptr (100  $\mu M$ ) in the absence of dGMP. Inset: Time dependence of the absorbance at 430 nm, with bi-exponential fitting (----) and residual analysis. b) Stern–Volmer plots of the quenching of the Ptr triplet states by dissolved  $O_2$ .  $\tau_T$  values were calculated by analyzing the transient absorbance  $\Delta A$  versus  $t$ ; excitation wavelength 355 nm, analysis wavelength 430 nm,  $[Ptr] = 100 \mu M$ .

tions for the quenching of both Ptr transients. The rate constants of quenching for each transient by dGMP were  $(2.0 \pm 0.6) \times 10^9$  and  $(5.4 \pm 0.8) \times 10^9$   $M^{-1} s^{-1}$  for the short- and long-lived Ptr transients, respectively. These results provide direct evidence for the interaction of both tautomeric triplet excited states of Ptr with dGMP.

Radical cations formed after the one-electron-oxidation of guanine nucleosides or nucleotides undergo fast deprotonation at  $pH > 5$ <sup>[36,37]</sup> and the resulting neutral radicals have been well characterized.<sup>[32,38]</sup> The formation of dGMP radical in solutions containing dGMP and Ptr upon UVA excitation has been reported.<sup>[19]</sup> Under our experimental conditions, the differential transient absorption spectra showed the narrow absorption band centered at 320 nm that is characteristic of 2'-deoxyguanosine radicals (Figure 5, lower inset). The formation of the neutral dGMP radical  $[dGMP(-H)^\cdot]$  can be monitored by the

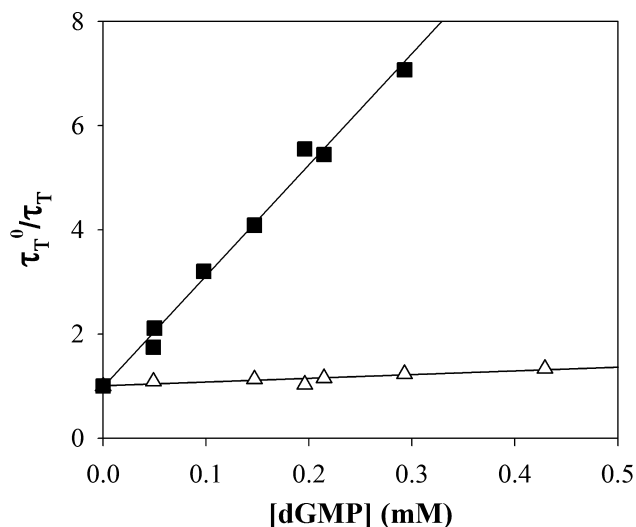


**Figure 4.** Stern–Volmer plots of the quenching of the Ptr triplet states by dGMP.  $\tau_T$  values were calculated by analyzing the transient absorbance  $\Delta A$  versus  $t$ ; excitation wavelength 355 nm, analysis wavelength 430 nm,  $[Ptr] = 100 \mu\text{M}$ .

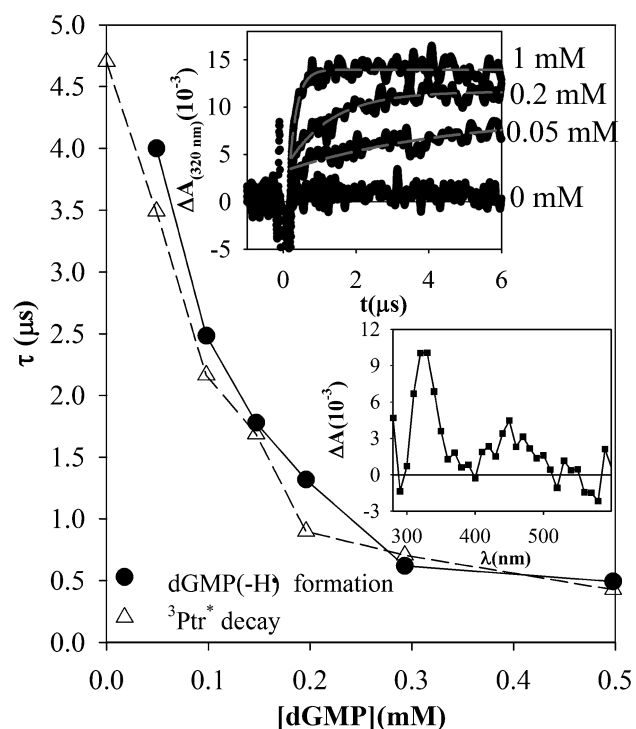


**Figure 5.** Lifetimes for the decay of the long-lived triplet state of Ptr and for the formation of the neutral radical dGMP(–H) $\cdot$  as a function of dGMP concentration. Experiments performed in Ar-saturated aqueous solutions, excitation wavelength: 355 nm,  $[Ptr] = 100 \mu\text{M}$ . Upper inset: Time dependence of the absorbance at 320 nm at various dGMP concentrations. Lower inset: Differential transient absorption spectra ( $\Delta A$ ), recorded after 10  $\mu\text{s}$  of the laser pulse, calculated as the difference between the spectra of Ptr with and without dGMP (2 mM).

time evolution of the  $\Delta A$  value at 320 nm after the laser pulse. In all cases, the traces recorded for different dGMP concentrations followed first-order kinetics and showed an increase in

the absorbance at infinite time with the dGMP concentration (Figure 5, upper inset). The lifetime value obtained for the formation of the dGMP radical decreased with nucleobase concentration and it was equal, within the experimental error, to that obtained for the decay of the long-lived triplet excited state of Ptr ( $^3Ptr^*$ ) at the corresponding dGMP concentration (Figure 5). Taking into account that the fluorescence lifetime of Ptr is 7.6 ns,<sup>[30]</sup> the participation of singlet excited states can be discarded and, consequently, the results indicate that the formation of the dGMP radical proceeds exclusively by electron transfer from the long-lived triplet excited states of Ptr.

In LFP experiments carried out at various  $O_2$  concentrations, for a given initial concentration of nucleobase (1 mM), it was observed that the higher the  $O_2$  concentration, the lower the dGMP(–H) $\cdot$  concentration reached after UVA excitation of Ptr (Figure S1 in the Supporting Information). In addition, the lifetime of the radical formation was reduced by  $O_2$  (Figure S1); growth lifetimes were 0.45, 0.38 and 0.15  $\mu\text{s}$ , in Ar, air- and  $O_2$ -saturated solutions, respectively.

Therefore, taking into account the results presented in this section, the mechanism represented by Reactions (1)–(7) can be proposed. After excitation of Ptr and formation of its triplet excited state by intersystem crossing (ISC),  $^3Ptr^*$  [Reactions (1) and (2)], several reaction pathways compete for the deactivation of the latter: unimolecular deactivation pathways [e.g. radiative and nonradiative energy losses, Reaction (3)], quenching by  $O_2$  [Reactions (4)], electron transfer from dGMP to yield the corresponding radical ions pair [Reaction (5)], and physical quenching by dGMP [Reaction (6)]. Note that  $k_{dGMP}^T$  determined in LFP experiments corresponds to the sum of the rate constants of Reactions (5) and (6) ( $k_{dGMP}^T = k_{ET-dGMP}^T + k_{q-dGMP}^T$ ). According to this reaction scheme, for a given initial concentration of dGMP, the amount of radicals formed depends on the  $O_2$  concentration due to the competition between Reactions (4) and (5).

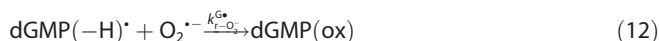


## 2.4. Reaction of the Guanine Neutral Radical

Once dGMP(–H) $\cdot$  reached a maximum concentration, its decay also depended on the  $O_2$  concentration (Figure S1). Under anaerobic conditions, the value of  $\Delta A$  at 320 nm and at other wavelengths was negligible at infinite time, suggesting that no secondary and/or final products were formed, which is consistent with the results of the continuous photolysis, that is, no consumption of dGMP was observed when  $O_2$ -free solutions

containing dGMP and Ptr were irradiated (Figure 2).<sup>[19]</sup> By contrast, the values of  $\Delta A$  at different wavelengths registered at infinite time in the presence of  $O_2$  suggest the formation of photoproducts, which agrees with the fact that consumption of the nucleotide was observed in steady-state experiments (Figure 2).<sup>[19]</sup>

The Ptr radical anion ( $Ptr^{\cdot-}$ ) can react with  $O_2$  to regenerate Ptr and produce  $O_2^{\cdot-}$  [Reaction (8)]. In turn,  $O_2^{\cdot-}$  can disproportionate with its conjugated acid  $HO_2^{\cdot}$  to form  $H_2O_2$  [Reaction (9)]. The neutral radical  $dGMP(-H)^{\cdot}$  can be reduced by  $Ptr^{\cdot-}$  to recover dGMP [Reaction (10)]. However, it has been reported that  $O_2^{\cdot-}$  reacts rapidly with guanine radicals according to two competitive mechanisms: chemical repair with the restoration of the guanine through electron transfer [Reaction (11)]<sup>[39,40]</sup> and addition, leading predominantly to the formation of 2,5-diamino-4H-imidazolone [Reaction (12)].<sup>[39–42]</sup> Alternatively,  $dGMP(-H)^{\cdot}$  may also react with  $O_2$  or other species present in the medium to yield oxidized products [dGMP(ox)] [Reaction (13)].



Under anaerobic conditions, radical recombination [Reaction (10)] is the only possible pathway to recovering the ground-state Ptr and dGMP molecules. Therefore, if  $dGMP(-H)^{\cdot}$  does not participate in another reaction, the total recombination of the radicals to completely recover the reactants should be observed. The kinetic traces recorded at 320 nm plotted as  $1/\Delta A$  versus time  $t$  are linear, and the half-life ( $t_{1/2}$ ) of the process increases with the decrease of the initial amount of  $dGMP(-H)^{\cdot}$  formed after the flash (Figure S2). This is confirmation that under anaerobic conditions the second-order recombination of  $dGMP(-H)^{\cdot}$  with  $Ptr^{\cdot-}$  is the single radical-scavenging reaction that occurs, and therefore no net reaction is observed.

Conversely, in the presence of dissolved  $O_2$ , Reactions (12) and (13) are significant pathways that compete with radical recombination [Reaction (10)]. In addition, Reaction (8) eliminates  $Ptr^{\cdot-}$ , contributing to a decrease of the rate of Reaction (10). The decays, measured in air-equilibrated solutions followed neither first- nor second-order kinetics. This observation can be explained by the fact that, under these experimental conditions,  $dGMP(-H)^{\cdot}$  is consumed through several pathways with different kinetics [Reactions (10)–(13)].

To investigate the role of  $O_2^{\cdot-}$  in the mechanism of dGMP photosensitization, LFP experiments in air-saturated solutions of Ptr and dGMP, with and without SOD, an enzyme that catalyzes Reaction (9), were carried out under otherwise identical conditions. The absorbance at infinite time was higher in the

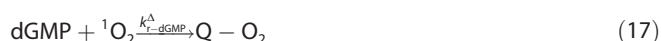
presence than in the absence of SOD (Figure S1), indicating that more degradation products are formed when  $O_2^{\cdot-}$  is quenched. This fact explains why during steady-state photolysis, consumption of dGMP was faster in the presence than in the absence of SOD (Figure 2).

A kinetic analysis of the reaction in the presence of SOD revealed that the decay of  $dGMP(-H)^{\cdot}$  followed a first-order rate law, as supported by the constant value of  $t_{1/2}$  at different initial amounts of  $dGMP(-H)^{\cdot}$  formed (Figure S3). This result is expected if it is assumed that Reaction (13) is the only one that results in the consumption of  $dGMP(-H)^{\cdot}$ , because in air-equilibrated solutions  $[O_2] \gg [dGMP(-H)^{\cdot}]$ , and the radical decays following a pseudo-first-order rate law. The same behavior would be observed if  $dGMP(-H)^{\cdot}$  reacted with other species of higher concentration, for example, with dGMP itself or with a photoproduct. Under these conditions it can be assumed that  $Ptr^{\cdot-}$  is fully scavenged by the excess of  $O_2$  to produce ground-state Ptr and  $O_2^{\cdot-}$  [Reaction (8)], which in turn, in the presence of SOD, is promptly dismutated to  $H_2O_2$  and  $O_2$  [Reaction (9)], thus avoiding the recovery of dGMP by Reaction (11).

## 2.5. Singlet Oxygen Studies

According to the hypotheses presented thus far, upon continuous irradiation the steady-state concentration of  $^1O_2$  produced by Ptr should be smaller in the presence of dGMP, not only because of quenching of  $^1O_2$  by dGMP itself, but also due to the quenching of  $^3Ptr^*$  by the nucleotide. In addition, the latter effect should depend on the  $O_2$  concentration. To explore this point, steady-state and time-resolved experiments were performed by irradiating Ptr at 340 nm in air- and  $O_2$ -saturated  $D_2O$  solutions at varying dGMP concentration and measuring the phosphorescence emission of  $^1O_2$  in the near-infrared (NIR) region.

The photosensitized formation of  $^1O_2$  by Ptr involves energy transfer from the  $^3Ptr^*$  to dissolved molecular oxygen [ $^3O_2$ ; Reaction (4)].<sup>[43]</sup> In turn,  $^1O_2$  relaxes to its ground state ( $^3O_2$ ) through solvent-induced radiationless and radiative pathways [Reactions (14) and (15)]. In the presence of dGMP,  $^1O_2$  may also be deactivated by bimolecular physical quenching [ $k_q^{\Delta}$ , Reaction (16)] and/or by oxidation of the quencher upon uptake of molecular oxygen [ $k_r^{\Delta}$ , Reaction (17)]. The rate constant for the total (physical and chemical) quenching of  $^1O_2$  by dGMP is the sum of these two processes ( $k_{dGMP}^{\Delta} = k_{q-dGMP}^{\Delta} + k_{r-dGMP}^{\Delta}$ ).



In time-resolved  $^1O_2$  phosphorescence experiments in  $D_2O$  solutions (pD 5.5), the observed decay at 1270 nm showed first-order kinetics in the presence of dGMP at various concentrations, either in air- or  $O_2$ -saturated solutions (Figure S4). As

the  $^1\text{O}_2$  lifetime ( $\tau_\Delta$ ) in  $\text{D}_2\text{O}$  solutions is much longer than that of  $^3\text{Ptr}^*$  ( $\tau_T$ ) under the experimental conditions used, the decay of the transient phosphorescence signal of  $^1\text{O}_2$  can be fitted with Equation (II):<sup>[44]</sup>

$$S_{(t)} = S_i \exp(-t/\tau_\Delta) \quad (\text{II})$$

where  $S_{(t)}$  is the signal measured by the NIR detector (proportional to the  $^1\text{O}_2$  concentration at a given time  $t$ ) and  $S_i$  is the pre-exponential factor (proportional to the initial  $^1\text{O}_2$  concentration at  $t=0$ , that is, at the end of the flash).

Considering only the dynamic component of the quenching of  $^1\text{O}_2$  by the nucleobase, the rate constant for the total quenching of  $^1\text{O}_2$  by dGMP,  $k_{\text{dGMP}}^\Delta$ , was calculated using Equation (III):

$$\frac{\tau_\Delta^0}{\tau_\Delta} = 1 + k_{\text{dGMP}}^\Delta \tau_\Delta^0 [\text{dGMP}] \quad (\text{III})$$

The values of  $k_{\text{dGMP}}^\Delta$  obtained from the corresponding plot (Figure 6a) were  $(1.0 \pm 0.2) \times 10^7$  and  $(7 \pm 4) \times 10^6 \text{ L mol}^{-1} \text{ s}^{-1}$  in  $\text{O}_2$ -saturated and air-equilibrated solutions. These values are closer to that previously published of  $(1.7 \pm 0.1) \times 10^7 \text{ L mol}^{-1} \text{ s}^{-1}$ , as the physical quenching contribution is almost negligible, that is,  $k_{\text{dGMP}}^\Delta \approx k_{T-\text{dGMP}}^\Delta$ .<sup>[19]</sup>

The initial phosphorescence intensity  $S_i$  of  $^1\text{O}_2$  decreased with the increase of dGMP concentration; this effect being much more pronounced in air than in  $\text{O}_2$ . This fact confirmed that the quenching of  $^3\text{Ptr}^*$  by dGMP [Reactions (5) and (6), Figure 4] efficiently competes with energy transfer from  $^3\text{Ptr}^*$  to  $^3\text{O}_2$ . Consequently, the efficiency of the energy transfer to  $\text{O}_2$  ( $\phi_{\text{et}}$ ) and thus the quantum yield of  $^1\text{O}_2$  production ( $\Phi_\Delta$ ) decrease as the dGMP concentration increases [Eq. (IV)]:

$$\Phi_\Delta = \Phi_T \phi_{\text{et}} = \Phi_T \frac{k_{\text{O}_2}^T [\text{O}_2]}{(k_d^T + k_{\text{O}_2}^T [\text{O}_2] + k_{\text{dGMP}}^T [\text{dGMP}])} \quad (\text{IV})$$

where  $\Phi_T$  is the quantum yield of  $^3\text{Ptr}^*$  formation,  $k_d^T$  [ $\text{s}^{-1}$ ] is the rate constant of  $^3\text{Ptr}^*$  deactivation in the absence of quencher [Reaction (3)],  $k_{\text{O}_2}^T$  [ $\text{L mol}^{-1} \text{ s}^{-1}$ ] is the rate constant of the energy transfer from  $^3\text{Ptr}^*$  to  $^3\text{O}_2$  [Reaction (4)] and  $k_{\text{dGMP}}^T = k_{\text{ET-dGMP}}^T + k_{\text{q-dGMP}}^T$  [ $\text{L mol}^{-1} \text{ s}^{-1}$ ] is the rate constant of  $^3\text{Ptr}^*$  total quenching by dGMP [Reactions (5) and (6)]. As the initial  $^1\text{O}_2$  emission signal  $S_i$  [Eq. (II)] is proportional to the initial  $^1\text{O}_2$  concentration, and therefore to  $\Phi_\Delta$ , the quenching efficiency of  $^3\text{Ptr}^*$  by dGMP can be evaluated from the Stern–Volmer analysis of the variation of  $S_i$  as a function of dGMP concentration [Eq. (V)]:

$$\frac{S_i^0}{S_i} = \frac{\Phi_\Delta^0}{\Phi_\Delta} = 1 + \tau_T k_{\text{dGMP}}^T [\text{dGMP}] \quad (\text{V})$$

where  $\tau_T$  ( $= \frac{1}{k_d^T + k_{\text{O}_2}^T [\text{O}_2]}$ ) is the lifetime of  $^3\text{Ptr}^*$  in the absence of dGMP under aerobic conditions. In agreement with Equation (V), the Stern–Volmer plots of  $S_i^0/S_i$  versus dGMP concen-

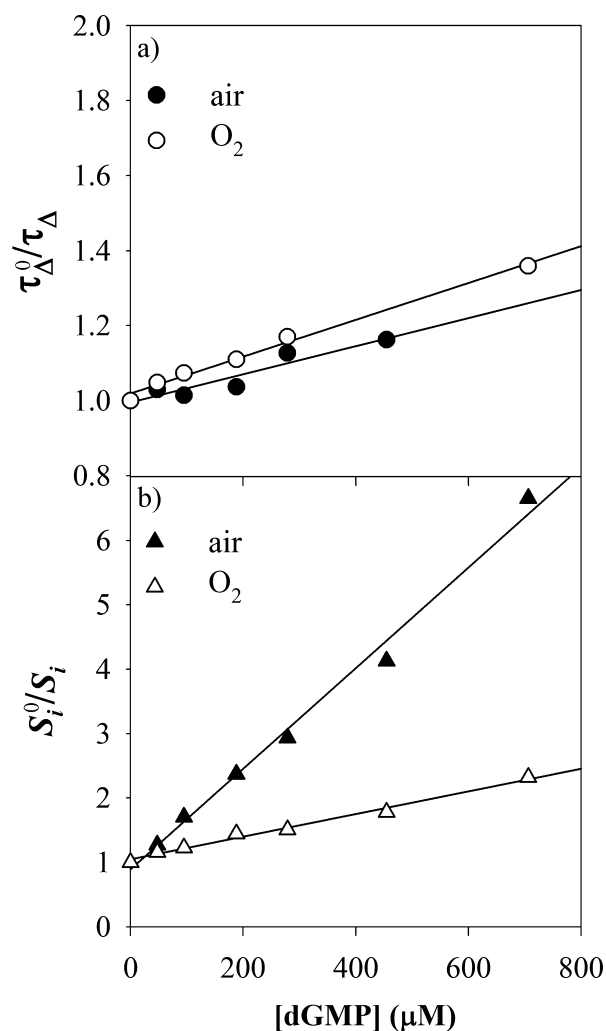


**Figure 6.** Time-resolved  $^1\text{O}_2$  experiments: quenching of  $^1\text{O}_2$  emission by dGMP. Experiments performed in  $\text{D}_2\text{O}$  solutions containing Ptr and dGMP at pD 5.5; excitation wavelength: 340 nm, [Ptr] = 200  $\mu\text{M}$ . a) Stern–Volmer plot of the  $^1\text{O}_2$  lifetimes ( $\tau_\Delta$ ), calculated by analyzing the NIR  $^1\text{O}_2$  luminescence decays [Eq. (III)]; b) Stern–Volmer plot of the initial  $^1\text{O}_2$  concentration, estimated using the pre-exponential factor [ $S_i$ , Eq. (II)].

tration were linear in air- and  $\text{O}_2$ -saturated solutions (Figure 6b). Taking into account the  $\tau_T$  values measured in air- and  $\text{O}_2$ -equilibrated aqueous solutions (1.4 and 0.4  $\mu\text{s}$ , respectively), calculation of  $k_{\text{dGMP}}^T$  from the slope of Stern–Volmer plots (Figure 6b), yielded values of  $(5 \pm 1) \times 10^9$  and  $(4 \pm 2) \times 10^9 \text{ L mol}^{-1} \text{ s}^{-1}$ , respectively. These values are equal, within the experimental error, to that obtained in LFP experiments (vide supra). Furthermore, and notably,  $k_{\text{dGMP}}^T$  values were about two orders of magnitude higher than  $k_{\text{dGMP}}^\Delta$  ( $\approx 1 \times 10^7 \text{ L mol}^{-1} \text{ s}^{-1}$ ).

In another set of experiments, the steady-state emission spectrum of  $^1\text{O}_2$  was recorded at constant Ptr concentration (200  $\mu\text{M}$ ) and different concentrations of dGMP (0–700  $\mu\text{M}$ ) at pD 5.5. As expected from the time-resolved experiments (Figure 6), a decrease in the  $^1\text{O}_2$  phosphorescence intensity ( $I_p$ ) resulted from an increase in the nucleobase concentration for both  $\text{O}_2$  concentrations, without a shift of the emission maximum wavelength (Figure S5). Again, the decrease in the emission was much more pronounced in air than in  $\text{O}_2$ .



Indeed, under continuous irradiation,  $I_p$  is proportional to the steady-state concentration of  $^1\text{O}_2$  ( $[^1\text{O}_2]_{ss}$ ). Taking into account the reactions involved in the production [Reactions (1), (2) and (4)] and quenching of  $^1\text{O}_2$  [Reactions (14)–(17)] and applying the quasi-stationary hypothesis to the concentrations of excited states,  $[^1\text{O}_2]_{ss}$  can be expressed as [Eq. (VI)]:

$$[^1\text{O}_2]_{ss} = q_{p,a} \Phi_{\Delta} \tau_{\Delta} \quad (\text{VI})$$

where  $q_{p,a}$  [ $\text{einstein L}^{-1} \text{s}^{-1}$ ] is the photon flux absorbed by the sensitizer.

In a given solvent at constant concentration of the sensitizer, that is, a constant photonic flux absorbed by Ptr, a Stern–Volmer analysis of the quenching of  $I_p$  by dGMP leads to the following relation [Eq. (VII)] by combining Equations (IV)–(VI):

$$\frac{I_p^0}{I_p} = \frac{[^1\text{O}_2]_{ss}^0}{[^1\text{O}_2]_{ss}} = \frac{\Phi_{\Delta}^0}{\Phi_{\Delta}} \times \frac{\tau_{\Delta}^0}{\tau_{\Delta}} \quad (\text{VII})$$

$$= (1 + \tau_1^0 k_{dGMP}^T [\text{dGMP}]) \times (1 + \tau_{\Delta}^0 k_{dGMP}^{\Delta} [\text{dGMP}])$$

where the superscript 0 refers to the values in the absence of dGMP in air-equilibrated or  $\text{O}_2$ -saturated solutions. In view of the values of the lifetimes and quenching rate constants, it is clear that the overall quenching of  $^1\text{O}_2$  emission will be dominated by the quenching of  $^3\text{Ptr}^*$  by dGMP and not by the quenching of  $^1\text{O}_2$  itself by dGMP; that is,  $\tau_{\Delta}^0 k_{dGMP}^{\Delta} \ll \tau_1^0 k_{dGMP}^T$ . The  $I_p^0/I_p$  ratios in air- and  $\text{O}_2$ -saturated solutions showed an upward curvature on a plot against dGMP concentration (Figure 7), which is expected for the quadratic dependence on the base concentration [Eq. (VII)]. In addition, values of  $I_p^0/I_p$  obtained from Equation (VII) are close to that obtained experimentally in steady-state  $^1\text{O}_2$  measurements (Figure 7).

### 3. Conclusions

We have used the photosensitized degradation of dGMP as a model reaction to present experimental evidence for a general mechanism that explains the photosensitizing action of pterins (Scheme 1), which can be described briefly as follows: after excitation of Ptr and formation of its triplet excited state ( $^3\text{Ptr}^*$ ); three reaction pathways compete for its deactivation, that is, intersystem crossing to a singlet ground state, energy transfer to  $\text{O}_2$ , which leads to regeneration of Ptr and formation of  $^1\text{O}_2$ ; finally, an electron-transfer reaction from dGMP to  $^3\text{Ptr}^*$  to form the dGMP radical cation ( $\text{dGMP}^{\cdot+}$ ), which immediately deprotonates to the corresponding dGMP neutral radical [ $\text{dGMP}(-\text{H})^{\cdot}$ ]. Under aerobic conditions, the electron transfer from  $\text{Ptr}^{\cdot-}$  to  $\text{O}_2$  regenerates Ptr and forms  $\text{O}_2^{\cdot-}$ , which in turn disproportionates to  $\text{H}_2\text{O}_2$ . The fate of the radical  $\text{dGMP}(-\text{H})^{\cdot}$  is strongly dependent on the presence of dissolved  $\text{O}_2$ . Under aerobic conditions  $\text{dGMP}(-\text{H})^{\cdot}$  can participate in three different pathways: 1) recombination with  $\text{Ptr}^{\cdot-}$  to recover dGMP and Ptr; 2) reduction by  $\text{O}_2^{\cdot-}$ ; 3) direct reaction with  $\text{O}_2$  to yield oxidation products.

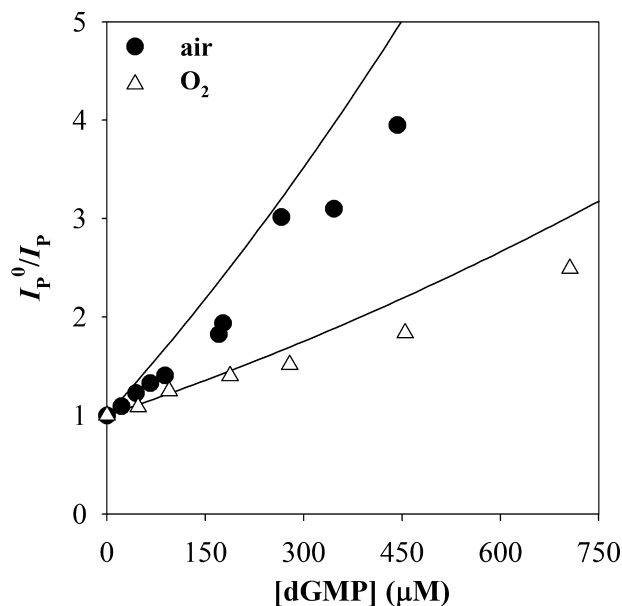
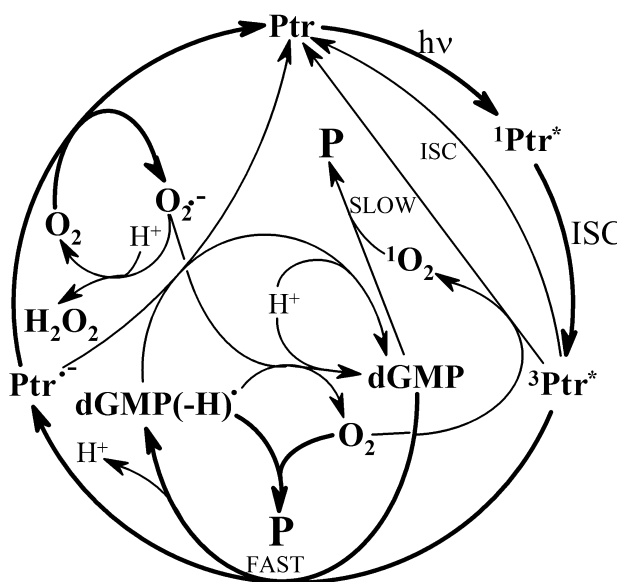


**Figure 7.** Steady-state  $^1\text{O}_2$  experiments showing quenching of the emission of  $^1\text{O}_2$  by dGMP, performed in  $\text{D}_2\text{O}$  solutions containing Ptr and dGMP at pD 5.5. Stern–Volmer plot of the integrated phosphorescence intensities ( $I_p$ ); points: experimental values obtained in air- (●) and  $\text{O}_2$ -saturated solutions (△). The solid lines represent the  $I_p^0/I_p$  values calculated with Equation (VI) using the estimated lifetimes and bimolecular rate constant values. Excitation wavelength 350 nm,  $[\text{Ptr}] = 200 \mu\text{M}$ .



**Scheme 1.** Mechanism of the degradation of dGMP photosensitized by Ptr. P: Products.

In contrast, under anaerobic conditions, only Pathway (1) is possible and no net reaction takes place. In air-equilibrated solutions, Reaction (3) is significant and degradation of dGMP takes place, which is faster if Pathway (2) is avoided by adding SOD to the solution. At high  $\text{O}_2$  concentrations ( $\text{O}_2$ -saturated solutions), the photosensitized reaction is slower than in air due to the quenching of  $^3\text{Ptr}^*$  by  $\text{O}_2$ .

Finally, although the reaction between dGMP and  $^1\text{O}_2$  takes place, its rate is much slower than that corresponding to the electron-transfer process and, consequently,  $^1\text{O}_2$  does not contribute significantly to dGMP consumption.

This model explains why and how a well-characterized  $^1\text{O}_2$  photosensitizer, such as Ptr, can photoinduce the degradation of a biomolecule by a type I instead of a type II mechanism, even though the biomolecule reacts efficiently with  $^1\text{O}_2$ . A kinetic analysis of the different pathways is the key to understand the mechanism. In particular, under our experimental conditions, the nucleotide reacts much faster with  $^3\text{Ptr}^*$  than with  $^1\text{O}_2$ . The main reason is that the rate constant of the first reaction is much larger than that of the second (i.e.  $k_{\text{dGMP}}^T \approx 100k_{\text{dGMP}}^A$ ). The other relevant point is that, surprisingly,  $\text{O}_2$  is not only needed as a source of  $^1\text{O}_2$ , but also to avoid the recombination of the radicals formed in the initial electron-transfer step. This model could be used to interpret results obtained with other related photosensitizers and with other substrates.

## Experimental Section

### General

Ptr was purchased from Schircks Laboratories (Jona, Switzerland) and used without further purification. Methanol was obtained from Mallinckrodt Chemical (Dublin, Ireland). dGMP, formic acid, SOD from bovine erythrocytes (lyophilized powder,  $\geq 95\%$  biuret,  $\geq 3000$  units per mg protein) and other chemicals were purchased from Sigma–Aldrich and used without further purification.

pH measurements were made using a PHM220 pH meter (Radiometer, Copenhagen, Denmark) combined with a pHC2011-8 electrode (Radiometer). The pH of the solutions was adjusted by adding small aliquots (few  $\mu\text{L}$ ) of aq. HCl or NaOH (0.1–2 M) using a micropipette.

### Steady-State Photolysis Experiments

Irradiation set-up: Aqueous solutions containing Ptr and dGMP were irradiated in 1 cm path length quartz cells at room temperature with a Rayonet RPR lamp (Southern New England Ultraviolet Co., Branford, CT) emitting at 350 nm (bandwidth  $\approx 20$  nm). Experiments with air-equilibrated solutions were performed in open quartz cells without bubbling, whereas Ar- and  $\text{O}_2$ -saturated solutions were obtained by bubbling the respective water-saturated gases (purity  $> 99.998\%$ ; Linde, La Plata, Argentina) for 20 min.

UV/Vis spectrophotometry: Electronic absorption spectra were recorded on a Shimadzu UV-1800 spectrophotometer, using quartz cells of 0.4 cm optical path length.

HPLC: A Prominence high-performance liquid chromatograph (Shimadzu) equipped with an SPD-M20A photodiode-array detector was used for monitoring the reaction. A Synergi Polar-RP column (ether-linked phenyl phase with polar endcapping,  $150 \times 4.6$  mm,  $4 \mu\text{m}$ , Phenomenex) was used for product separation. Solutions containing 3% methanol and 97% aq. formic acid (25 mm, pH 3.2) were used as the mobile phase.

### Transient Absorption Experiments

LFP experiments were performed as described elsewhere.<sup>[20,45]</sup> In brief, Ptr was excited with the third harmonic at 355 nm of a Nd:YAG Minilite II laser (7 ns full width at half maximum, 7 mJ per pulse; Continuum, Santa Clara, CA, USA). The transient absorption spectra were recorded with the *m*-LFP 112 apparatus (Luzchem, Ottawa, Canada) linked to a 300 Mhz Tektronik TDS 3032B digital oscilloscope for signal acquisition. Signal analysis was performed using OriginPro 8.0 software (OriginLab Corporation).

### Singlet Oxygen Studies

The experiments were performed at room temperature using a NIR PMT Module H10330-45 (Hamamatsu, Iwata City, Japan) coupled to FL3 TCSPC-SP (Horiba Jobin Yvon) single-photon-counting equipment, as described elsewhere.<sup>[28]</sup>  $\text{D}_2\text{O}$  was used as a solvent as the lifetime of  $^1\text{O}_2$  ( $\tau_A$ ) is longer in  $\text{D}_2\text{O}$  than in  $\text{H}_2\text{O}$ .<sup>[46,47]</sup>

Steady-state experiments: The sample solution in a quartz cell was irradiated with a CW 450W Xe source equipped with an excitation monochromator. The luminescence, after passing through an emission monochromator, was detected at  $90^\circ$  with respect to the incident beam using the NIR photomultiplier tube. Corrected emission spectra obtained by excitation at 340 nm were recorded between 950 and 1400 nm, and the total integrated  $^1\text{O}_2$  phosphorescence intensities ( $I_p$ ) were calculated by integration of the emission band.

Time-resolved experiments: An FL-1040 phosphorimeter (Horiba, Jovin Ivon, New Jersey, United States) was used and the tail of the phosphorescence decays of  $^1\text{O}_2$  was collected after 50  $\mu\text{s}$  of the lamp pulse. The emission at 1270 nm was recorded as a function of time.

### Acknowledgements

This work was partially supported by CONICET (grants PIP 112-200901-00425 and PIP 0374/12), ANPCyT (grant PICT 12-2666), UNLP (grant X586), and UNSE (grant 23A/162). M.P.S. thanks CONICET for a doctoral research fellowship. C.L., C.D.B. and A.H.T. are research members of CONICET.

**Keywords:** 2'-deoxyguanosine 5'-monophosphate • electron transfer • guanine radicals • photosensitization • pterin

- [1] S. E. Braslavsky, *Pure Appl. Chem.* **2007**, *79*, 293–465.
- [2] J. Cadet, T. Douki, J.-L. Ravanat, P. Di Mascio, *Photochem. Photobiol. Sci.* **2009**, *8*, 903–911.
- [3] F. El Ghissassi, R. Baan, K. Straif, Y. Grosse, B. Secretan, V. Bouvard, L. Benbrahim-Tallaa, N. Guha, C. Freeman, L. Galichet, V. Coglianò, *Lancet Oncol.* **2009**, *10*, 751–752.
- [4] T. B. H. Buckel, A. M. Goldstein, M. C. Fraser, B. Rogers, M. A. Tucker, *Arch. Dermatol.* **2006**, *142*, 485–488.
- [5] W. Ting, K. Schultz, N. N. Cac, M. Peterson, H. W. Walling, *Int. J. Dermatol.* **2007**, *46*, 1253–1257.
- [6] J. Moan, A. C. Porojnicu, A. Dahiback, *Adv. Exp. Med. Biol.* **2008**, *624*, 104–116.
- [7] F. Manjón, L. Villén, D. García-Fresnadillo, G. Orellana, *Environ. Sci. Technol.* **2008**, *42*, 301–307.
- [8] F. Manjón, D. García-Fresnadillo, G. Orellana, *Photochem. Photobiol. Sci.* **2009**, *8*, 926–932.
- [9] A. P. Castano, P. Mroz, M. R. Hamblin, *Nat. Rev. Cancer* **2006**, *6*, 535–545.
- [10] P. Babilas, S. Schreml, M. Landthaler, R.-M. Szeimies, *Photodermatol. Photoimmunol. Photomed.* **2010**, *26*, 118–132.

- [11] J. Cadet, E. Sage, T. Douki, *Mutat. Res.* **2005**, *571*, 3–17.
- [12] S. Mouret, C. Baudouin, M. Charveron, A. Favier, J. Cadet, T. Douki, *Proc. Natl. Acad. Sci. USA* **2006**, *103*, 13765–13770.
- [13] C. S. Foote, *Photochem. Photobiol.* **1991**, *54*, 659.
- [14] A. Karotki, M. Khurana, J. R. Lepock, B. C. Wilson, *Photochem. Photobiol.* **2006**, *82*, 443–452.
- [15] M. C. De Rosa, R. J. Crutchley, *Coord. Chem. Rev.* **2002**, *351*, 233–234.
- [16] J. Cadet, J.-L. Ravanat, G. R. Martinez, M. H. G. Medeiros, P. Di Mascio, *Photochem. Photobiol.* **2006**, *82*, 1219–1225.
- [17] P. R. Ogilby, *Chem. Soc. Rev.* **2010**, *39*, 3181–3209.
- [18] D. I. Pattison, A. S. Rahmantoa, M. J. Davies, *Photochem. Photobiol. Sci.* **2012**, *11*, 38–53.
- [19] G. Petroselli, M. L. Dántola, F. M. Cabrerizo, A. L. Capparelli, C. Lorente, E. Oliveros, A. H. Thomas, *J. Am. Chem. Soc.* **2008**, *130*, 3001–3011.
- [20] M. P. Serrano, C. Lorente, F. E. Morán Vieyra, C. D. Borsarelli, A. H. Thomas, *Phys. Chem. Chem. Phys.* **2012**, *14*, 11657–11665.
- [21] A. H. Thomas, M. P. Serrano, V. Rahal, P. Vicendo, C. Claparols, E. Oliveros, C. Lorente, *Free Radical Biol. Med.* **2013**, *63*, 467–475.
- [22] C. Castaño, M. L. Dántola, E. Oliveros, A. H. Thomas, C. Lorente, *Photochem. Photobiol.* **2013**, *89*, 1448–1455.
- [23] E. A. Lissi, M. V. Encinas, E. Lemp, M. A. Rubio, *Chem. Rev.* **1993**, *93*, 699–723.
- [24] M. P. Denofrio, S. Hatz, C. Lorente, F. M. Cabrerizo, P. R. Ogilby, A. H. Thomas, *Photochem. Photobiol. Sci.* **2009**, *8*, 1539–1549.
- [25] E. Oliveros, P. Suardi-Muraseco, T. Aminian-Saghafi, A. M. Braun, H.-J. Hansen, *Helv. Chim. Acta* **1991**, *74*, 79–90.
- [26] R. Schmidt, C. Tanielian, R. Dunsbach, C. Wolff, *J. Photochem. Photobiol. A* **1994**, *79*, 11–17.
- [27] C. Martí, O. Jürgens, O. Cuenca, M. Casals, S. Nonell, *J. Photochem. Photobiol. A* **1996**, *97*, 11–18.
- [28] C. Lorente, E. Arzoumanian, C. Castaño, E. Oliveros, A. H. Thomas, *RSC Adv.* **2014**, *4*, 10718–10727.
- [29] I. Fridovich, *Photochem. Photobiol.* **1978**, *28*, 733–741.
- [30] C. Lorente, A. H. Thomas, *Acc. Chem. Res.* **2006**, *39*, 395–402.
- [31] L. P. Candeias, S. Steenken, *J. Am. Chem. Soc.* **1992**, *114*, 699–704.
- [32] Y. Rokhlenko, N. E. Geacintov, V. Shafirovich, *J. Am. Chem. Soc.* **2012**, *134*, 4955–4962.
- [33] C. Chahidi, M. Aubailly, A. Momzikoff, M. Bazin, R. Santus, *Photochem. Photobiol.* **1981**, *33*, 641–649.
- [34] J. W. Ledbetter, W. Pfeleiderer, J. H. Freisheim, *Photochem. Photobiol.* **1995**, *62*, 71–81.
- [35] J. W. Ledbetter, W. Pfeleiderer, J. H. Freisheim, in *Chemistry and Biology of Pteridines and Folates*, Vol. 338 (Eds.: J. Ayling, M. G. Nair, C. Baugh), Plenum Press, New York, **1993**, pp. 499–502.
- [36] L. P. Candeias, S. Steenken, *J. Am. Chem. Soc.* **1989**, *111*, 1094–1099.
- [37] S. Steenken, *Chem. Rev.* **1989**, *89*, 503–520.
- [38] C. Chatgililoglu, M. D'Angelantonio, G. Kciuk, K. Bobrowski, *Chem. Res. Toxicol.* **2011**, *24*, 2200–2206.
- [39] R. Misiaszek, C. Crean, A. Joffe, N. E. Geacintov, V. Shafirovich, *J. Biol. Chem.* **2004**, *279*, 32106–32115.
- [40] M. Al-Sheikhly, *Radiat. Phys. Chem.* **1994**, *44*, 297–301.
- [41] J. Cadet, T. Douki, J.-L. Ravanat, *Acc. Chem. Res.* **2008**, *41*, 1075–1083.
- [42] V. Shafirovich, J. Cadet, D. Gasparutto, A. Dourandin, N. E. Geacintov, *Chem. Res. Toxicol.* **2001**, *14*, 233–241.
- [43] E. Cadenas, *Annu. Rev. Biochem.* **1989**, *58*, 79–110.
- [44] S. Nonell, S. E. Braslavsky, *Methods Enzymol.* **2000**, *319*, 37–49.
- [45] L. Valle, F. E. Morán Vieyra, C. D. Borsarelli, *Photochem. Photobiol. Sci.* **2012**, *11*, 1051–1061.
- [46] P. R. Ogilby, C. S. Foote, *J. Am. Chem. Soc.* **1983**, *105*, 3423–3430.
- [47] F. Wilkinson, H. P. Helman, A. B. Ross, *J. Phys. Chem. Ref. Data* **1995**, *24*, 663–677.

---

Received: March 13, 2015

Published online on May 28, 2015